THE JOURNAL OF BIOLOGICAL CHEMISTRY
Vol. 273, No. 24, Issue of June 12, pp. 15061–15068, 1998

Printed in U.S.A.

The Human Proteinase-activated Receptor-3 (PAR-3) Gene

IDENTIFICATION WITHIN A PAR GENE CLUSTER AND CHARACTERIZATION IN VASCULAR ENDOTHELIAL CELLS AND PLATELETS*

(Received for publication, March 13, 1998)

Valentina A. Schmidt‡, William C. Nierman§, Donna R. Maglott§, Lisa D. Cupit‡, Keith A. Moskowitz¶, Jean Ann Wainer‡, and Wadie F. Bahou‡‖**

From the ‡Department of Medicine, State University of New York at Stony Brook, Stony Brook, New York 11794, the §Department of Molecular Biology, American Type Culture Collection, Manassas, Virginia 20110, ¶Accumetrics Inc., San Diego, California 92121, and ‖Program in Genetics, State University of New York at Stony Brook, Stony Brook, New York 11794

Proteolytically activated receptors (PARs) represent an emerging subset of seven transmembrane G protein-coupled receptors that mediate cell activation events by receptor cleavage at distinct scissile bonds located within receptor amino termini. Differential genomic blotting using a yeast artificial chromosome known to contain the PAR-1 and PAR-2 genes identified the PAR-3 gene within a PAR gene cluster spanning ~100 kilobases at 5q13. The PAR-3 gene is relatively small (~12 kilobases); and, like the PAR-1 and PAR-2 genes, it displays a two-exon structure, with the majority of the coding sequence and the proteolytic cleavage site contained within the larger second exon. Sequence analysis of the 5′-flanking region demonstrates that the promoter is TATA-less, similar to that seen with PAR-1, with the identification of nucleic acid motifs potentially involved in transcriptional gene regulation, including AP-1, GATA, and octameric sequences. PAR-3 transcripts were apparent in human vascular endothelial cells, although at considerably lower levels than those of PAR-1 and not significantly modulated by the endothelial cell stimulus tumor necrosis factor-α. Likewise, although PAR-3 mRNA was evident in human platelets, receptor cell surface expression was modest (~10%) compared with that of PAR-1. Thus, although PAR-3 is postulated to represent a second thrombin receptor, its modest endothelial cell and platelet expression suggest that PAR-3 activation by α-thrombin is less relevant for physiological responses in these mature cells. Rather, given its disparately greater expression in megakaryocytes (and megakaryocyte-like human erythroleukemia cells), a regulatory role in cellular development (by protease activation) could be postulated.

Proteolytically activated receptors (PARs)[1] are members of a larger family of seven transmembrane cell surface receptors that mediate cell activation events through heterotrimeric G proteins (1, 2). Until very recently, two PARs had been isolated to date, the thrombin receptor (PAR-1) (3) and the proteinase-activated receptor (PAR-2) (4, 5). Unlike the former class of receptors in which cellular activation events are initiated by standard receptor-ligand binding interactions, both PAR-1 and PAR-2 are activated by cleavage at distinct Arg-Ser bonds located within the NH_2-terminal extension of both receptors, and synthetic peptidomimetics representing the new NH_2 terminus after receptor cleavage function as full receptor agonists irrespective of receptor cleavage. In addition to displaying similar molecular mechanisms of receptor activation, functional similarities between PAR-1 and PAR-2 have also been observed. Thus, both are expressed on vascular endothelial cells (6), and both mediate proliferative responses when activated by their protease agonists (7, 8) or synthetic peptide ligands (6, 8). These structure/function similarities also extend to the gene level; thus, both PAR-1 and PAR-2 genes are known to co-localize at 5q13, and both genes are organized similarly, suggesting evolution from a common ancestral gene (9).

Given evolving evidence for protease activation of multiple cell types (2, 7) and the corollary that some, if not all, of these cellular sequelae may be mediated by activation of novel PARs, we adapted a positional cloning approach as a strategy for the identification of other putative PARs that may co-cluster within this region of the genome. Interestingly, we identified the recently characterized PAR-3 gene (10) within this region of the genome and demonstrate that its structural organization is essentially identical to that of PAR-1 and PAR-2, reinforcing the concept of a gene family of receptors evolving from a common ancestral gene and emerging along a distinct evolutionary pathway. Furthermore, like PAR-1 and PAR-2, PAR-3 is also expressed on vascular endothelial cells, although at considerably lower levels; similar low level but detectable PAR-3 expression is also evident in human platelets; thus, although PAR-3 appears to be a second "thrombin receptor," its comparatively modest expression in these cell types suggests a functional role distinct from PAR-1 in mediating cell activation events by α-thrombin.

MATERIALS AND METHODS

Supplies, Reagents, and Cell Lines—Restriction enzymes were purchased from Stratagene (La Jolla, CA) or New England Biolabs (Beverly, MA). Avian myeloblastosis virus reverse transcriptase was from Seikagaku America, Inc. (Rockville, MD), and Expand™ long template polymerase was from Boehringer Mannheim. Oligonucleotide primers

* This work was supported by National Institutes of Health Grant HL49141 and an American Heart Association Established Investigator award (to W. F. B). The costs of publication of this article were defrayed in part by the payment of page charges. This article must therefore be hereby marked "*advertisement*" in accordance with 18 U.S.C. Section 1734 solely to indicate this fact.

The nucleotide sequence(s) reported in this paper has been submitted to the GenBank™/EBI Data Bank with accession number(s) AF050525.

** To whom correspondence should be addressed: Division of Hematology, HSC T15-040, SUNY, Stony Brook, NY 11794-8151. Tel.: 516-444-2059; Fax: 516-444-7530; E-mail: Wbahou@mail.som.sunysb.edu.

[1] The abbreviations used are: PAR(s), proteolytically activated receptor(s); HUVEC, human umbilical vein endothelial cell(s); HEL, human erythroleukemia cell(s); YAC, yeast artificial chromosomal; kb, kilobase(s); RH, radiation hybrid; PCR, polymerase chain reaction; bp, base pair(s); BSA, bovine serum albumin; FITC, fluorescein isothiocyanate; PBS, phosphate-buffered saline.

were synthesized on an Applied Biosystems model 381A single-channel synthesizer (G. D'Angelo, Molecular Biology Core, SUNY Stony Brook). Human umbilical vein endothelial cells (HUVEC) were isolated from pooled primary cultures of human umbilical veins and propagated as described previously (6). Human erythroleukemia (HEL) cells were propagated in RPMI medium supplemented with 10% fetal calf serum, 100 units/ml penicillin, and 100 μg/ml streptomycin.

Genomic Analysis and Library Screening—Total genomic DNA from normal human volunteers was extracted from peripheral blood leukocytes as described previously (9) and quantitated by absorption spectrophotometry at 260 nm. Approximately 5–10 μg of DNA was digested with various restriction enzymes for Southern blot analysis. The separation of large DNA fragments on agarose gels was completed using an inversion field gel electrophoresis apparatus (Switchback™ pulse controller, Hoefer Scientific Instruments, San Francisco). Yeast artificial chromosomal (YAC) DNA was isolated as described previously (11), and human genomic fragments were separated from yeast chromosomes using a 1% agarose gel in 0.5 × TBE (Tris borate-EDTA), run at 6.9 V/cm in 0.5 × TBE buffer at 10 °C with a pulse timer of 1–50 s and a forward/reverse ratio of 3:1 for 24 h. Gels were blotted onto nylon membranes (Schleicher & Schuell) and hybridized to ^{32}P-radiolabeled cDNA probes. Blots were washed at high (0.1 × SSC, 0.1% SDS, 1 mM EDTA, pH 8.0, and 10 mM sodium phosphate at 68 °C for 1 h) or low (0.1 × SSC, 0.5% SDS, 1 mM EDTA, pH 8.0, 10 mM sodium phosphate at 55 °C for 30 min) stringency and analyzed by autoradiography with Kodak XAR-5 film with an intensifying screen at −80 °C for 3–10 days. For some experiments, filters were stripped according to the manufacturer's recommendations and adequacy confirmed by overnight autoradiography.

The PAR-3 cDNA was isolated from a HUVEC cDNA library cloned into the bacteriophage vector λgt11, essentially as described previously (6). Positive phage clones were plaque purified, and the DNA was purified from minilysates by standard methods (9). The PAR-3 gene was isolated from a cosmid library generated from the ~1.4-megabase YAC 798D11, shown previously in this laboratory to contain both PAR-1 and PAR-2 genes (11). A size-selected library ranging from ~30 to ~40 kb was generated by partial *Mbo*I digestion of 1 μg of YAC 798D11 DNA followed by ligation to SuperCos-1 vector (Stratagene) containing flanking *Bam*HI sites. Ligation products were packaged using 25 μl of Gigapack III XL packaging extract for 2 h at 25 °C followed by titering and amplification using *Escherichia coli* host strain XL1-Blue. The titer of the unamplified library was ~1×10^5 colony-forming units/ml, consistent with a ~10^3-fold representation of nucleotide sequences. Library screening was completed using the ^{32}P-radiolabeled PAR-3 cDNA as probe, and DNA from individual cosmids was characterized further by extensive restriction mapping. Discrete genomic fragments were gel purified and ligated into pBluescript (Stratagene) for DNA sequence analysis using dideoxy chain termination. Exon-intron boundaries were defined by comparison of the genomic DNA sequence with that of the published cDNA (10). Sequence analysis was performed using the Wisconsin Genetics Computer Group Package (12). The identification of PAR-3 promoter nucleotide motifs potentially involved in transcriptional gene regulation was characterized using TRANSFAC software (13).

Radiation Hybrid (RH) Mapping Analysis—Genetic mapping within the PAR gene cluster was completed using both the Stanford G3 (~500-kb resolution) and TNG3 (~100-kb resolution) RH mapping panels (11, 14). PCR screening was completed using the following PAR-3-specific oligonucleotide primers: PAR2064 (5′–3′: TCCATCCTTTCACCTACCGGG, bp 731–751) and PAR2065 (5′–3′: TAGCAGTAGATGATAAGCACA, bp 989–969) (10). PAR-1, PAR-2, and microsatellite-specific primers encompassing this region of the genome were as described previously (11). PCR conditions were optimized for individual primer pairs, but the thermal profile generally included a 1-min 95 °C denaturation step, a 2-min 55 °C annealing step, a 3-min 72 °C primer extension step, with a final extension for 10 min at 72 °C; after 25 cycles in a thermocycler (Coy Laboratory Products, Ann Arbor, MI), products were analyzed by Southern blot analysis in a 3% ethidium-stained agarose gel and scored as present or absent. Retention patterns were submitted for two-point linkage analyses to the server maintained by

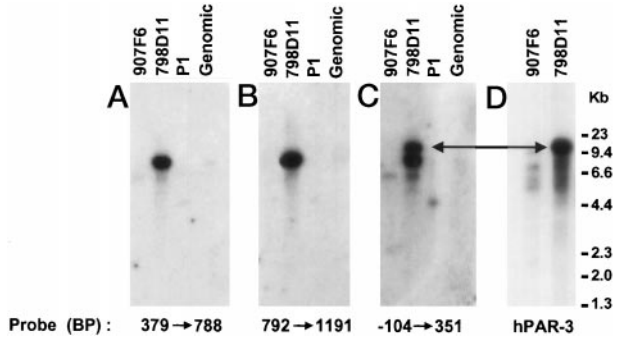

FIG. 1. **Identification of the human PAR-3 gene within a PAR gene cluster.** 1 μg of DNA from YAC 798D11, YAC 907F6 (known to contain the D5S424 microsatellite marker but not PAR-1 or PAR-2 genes (9)), P1–4251 (an anonymous P1 genomic clone (9)), or 10 μg of human genomic DNA was digested with *Eco*RI for Southern blot analysis using the ^{32}P-radiolabeled PCR fragments spanning discrete portions (in base pairs, *BP*) of the PAR-2 cDNA (*panels A–C*). Blots were washed to low stringency to maximize hybridization to homologous sequences. A distinct ~16-kb fragment is evident only in YAC 798D11 using a 5′-probe (*panel C*, *arrow*), which is not evident using other probes, consistent with a homologous gene residing within this portion of the genome. Rehybridization of the blot with the hPAR-3 cDNA (λ2B1A, see Fig. 4) identified this band as human PAR-3 (*panel D*, high stringency wash). The PAR-2-specific ~9-kb band was evident in genomic DNA after longer exposure (not shown). Size markers using *Hin*dIII-digested λ DNA are shown.

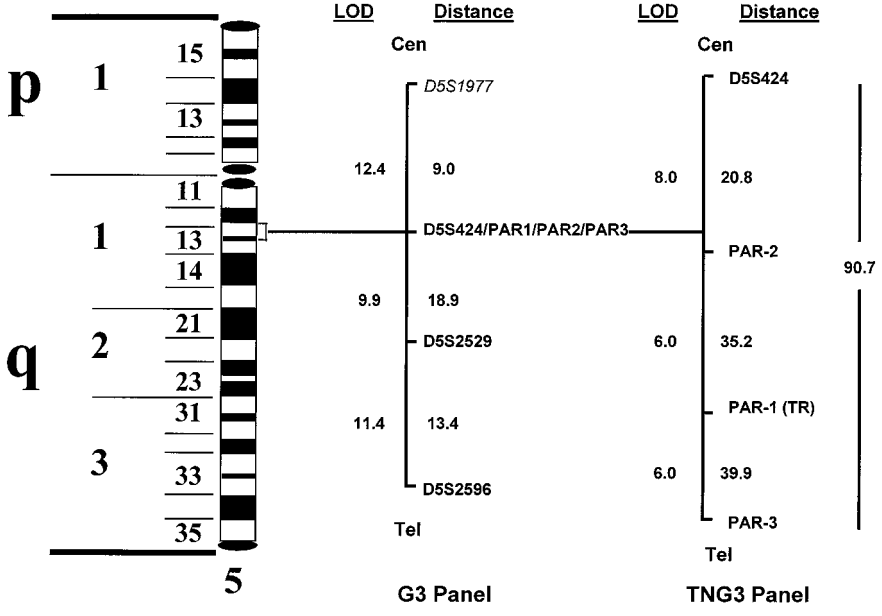

FIG. 2. **Schema of human chromosome 5 with interorder distances for PAR genes.** PAR-1-, PAR-2-, and PAR-3-specific oligonucleotide primers were used for determination of amplification (and retention) patterns using both G3 and TNG3 RH panels, followed by two-point linkage analysis using RH2PT (16). The centromeric/telomeric representation is a consensus from previous mapping data utilizing SHGC G3 RH panel; the position of D5S1977 relative to D5S424 and D5S2529 has not been confirmed in this laboratory and thus is presented in *italics* (11). Arbitrary distance measurements are expressed as cR_8000 (8,000 centiRad, the radiation dosage used for the generation of the *G3 panel*) or cR_50,000 (*TNG3 panel*). Note that distance estimates from the two panels are not comparable and do not indicate physical distances but simply reflect more frequent radiation-induced chromosomal breakage events. *Tel*, telomere; *Cen*, centromere; *LOD*, log of odds.

A

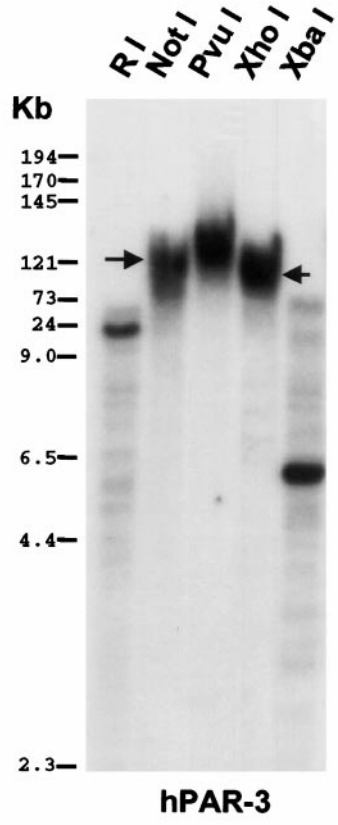

B

	EcoR I	Xba I	Xho I	Not I
hPAR-1	5.5;2.8	~8	~90	~120
hPAR-2	~9	~16	~90	~120
hPAR-3	~16	~6	~90	~120

FIG. 3. **Characterization of the PAR gene cluster by inversion field gel electrophoresis.** *Panel A*, 1 μg of YAC 798D11 DNA was digested with *Eco*RI (*first lane* from *left*), *Not*I (*second lane*), *Pvu*I (*third lane*), *Xho*I (*fourth lane*), or *Xba*I (*fifth lane*) for Southern blot analysis using the ^{32}P-radiolabeled PAR-3 cDNA (λ2B1A) as probe followed by high stringency wash and overnight autoradiography. The table (*panel B*) delineates the restriction fragment sizes when the blot was stripped and sequentially hybridized with the cDNAs for PAR-1 (20) and PAR-2 (6). As demonstrated, all three genes are contained within the identical *Not*I (~120 kb) or *Xho*I (~90 kb) fragments. Note the different sized restriction patterns with *Xba*I or *Eco*RI, excluding the possibility that the cDNAs are cross-hybridizing to other genes within the cluster.

the Stanford Human Genome Center[2] or analyzed using RHMAP (version 2.02), a software package for multipoint radiation hybrid mapping (16).

RNA Preparation and Northern and PCR Analysis—Confluent HUVEC in second to fifth passage were harvested directly with a rubber policeman, and total cellular RNA was isolated by immediate solubilization in guanidine hydrochloride and serial ethanol precipitation (6). Alternatively, poly(A) mRNA was isolated from solubilized HUVEC (or HEL cells) by oligo(dT)-cellulose chromatography (Invitrogen, San Diego). For some experiments, 3×10^7 HUVEC were stimulated with 100 units/ml tumor necrosis factor-α (17) for 4 or 24 h followed by RNA isolation. Transcript expression of murine tissues was completed using 1 μg of poly(A) RNA (Clontech, Palo Alto, CA). Northern blot analysis was completed by size fractionation in a 1% denaturing agarose gel, and equivalent RNA loading was confirmed by reprobing with a γ-actin cDNA probe (18). Reverse transcription-PCR was completed by incubating ~1 μg of total cellular RNA with 1 μg of a 14-mer oligo(dT) primer at 41 °C for 1 h using 10 units of avian myeloblastosis virus reverse transcriptase in a solution containing 50 mM Tris/HCl, pH 8.3, 50 mM KCl, 8 mM $MgCl_2$, 10 mM dithiothreitol, and 500 μM individual dNTPs in a final volume of 50 μl. 10 μl was subsequently adjusted to PCR conditions using approximately 0.01 OD unit of each PCR primer and 5 units of *Taq* polymerase (*Thermus aquaticus* DNA polymerase; Perkin-Elmer). Oligonucleotide primers included the reverse primer PAR2065 (see above) and the forward primers PAR2066 (5′–3′: ATAACGTTTAAGAGACGGGACT, bp 111–132). PCR conditions included a 1-min 15-s denaturation step at 94 °C, a 1-min 55 °C annealing step, and a 3-min primer extension step at 72 °C. Amplifications consisted of 35 rounds using a DNA thermocycler, and insert sizes were determined by electrophoresis in a 1% ethidium-stained agarose gel. Platelet PCR was completed in a similar manner, except for minor modifications, essentially as described previously (19).

PAR-3 Immunodetection—A 17-mer peptide encompassing the PAR-3 cleavage site with an added NH_2-terminal cysteine and COOH-terminal amide (PAR-3^{32-48}, Ac-CKPTLPIKTFRGAPPNS-amide) was custom synthesized by Quality Controlled Biochemicals (Hopkington, MA) and purified by reverse phase high pressure liquid chromatography. For antibody generation, the peptide was conjugated to keyhole limpet hemocyanin or to BSA using the hetero-bifunctional cross-linking reagent mal-sac HNSA, and the keyhole limpet hemocyanin-conjugate was used to immunize New Zealand White rabbits. Immunoreactivity of the anti-PAR-3 antibody to the BSA conjugate was confirmed by solid phase enzyme-linked immunosorbent assay. Preimmune and immune rabbit IgGs were purified by protein G affinity chromatography. For immunofluorescent studies, the immunopurified IgG was labeled directly with FITC (0.2 mg of FITC/mg of IgG) in 0.1 M sodium carbonate buffer, pH 9.5, for 2 h at 25 °C, and unbound FITC was removed by gel filtration on a Bio-Rad 10-DG column developed with degassed PBSA (10 mM sodium phosphate, 150 mM sodium chloride, 0.05% sodium azide, pH 7.4).

Immunofluorescent staining of confluent HUVEC was completed in eight-well chamber slides after fixation in 4% paraformaldehyde for 20 min at 25 °C (for determination of cell surface staining) or fixation and permeabilization using ice-cold 100% acetone for 60 s. Fixed HUVEC were then washed extensively with PBS followed by incubation with 100 μg/ml FITC-conjugated anti-PAR-3 IgG or a 1:100 dilution of the FITC-conjugated IgG alone for 60 min at 4 °C. After the last of five washes in PBS, cells were mounted in Aquamount, and fluorescent images were obtained using a Nikon Diaphot inverted microscope equipped with fluorescent optics (Nikon, Garden City, NY). Images were frame averaged to 256 frames with Image I software (Universal Imaging, Media, PA) using laser light excited at 529 nm and a blocking filter of 550 nm. Flow cytometric analysis of HUVEC was completed by detaching adherent cells using PBS and 10 mM EDTA and resuspending the cells to a final concentration of 5×10^5/ml PBS and 0.1% BSA. 200-μl aliquots were then incubated with 100 μg/ml FITC-conjugated anti-PAR-3 IgG for 60 min at 4 °C in PBS and 0.1% BSA, and cells were washed twice and then fixed in 1% formalin before analysis.

Platelet cell surface PAR-1/PAR-3 expression was completed as described previously (20). Briefly, platelet-rich plasma was prepared in 10 mM EDTA from healthy human donors by differential centrifugation and adjusted to 3×10^8 platelets/ml TSE (0.1 M Tris, 0.15 M NaCl, 10 mM EDTA, pH 7.4). 400-μl aliquots were then incubated with 100 μg/ml FITC-conjugated anti-PAR-3 IgG, 100 μg/ml anti-PAR-1 IgG (20), or 100 μg/ml nonimmune rabbit IgG for 30 min at 25 °C. For PAR-1 expression, platelets were incubated with a 1:100 dilution of the FITC-conjugated goat anti-rabbit $F(ab')_2$ secondary antibody (Tago, Inc., Burlingame, CA) for 20 min at 25 °C; samples were then washed three times in TSE, fixed in 1% formalin, and analyzed in a FACStar flow cytometer (Becton Dickinson and Co., Rutherford, NJ).

RESULTS AND DISCUSSION

Identification of the Human PAR-3 Gene within the PAR Gene Cluster—Previous work from this laboratory demonstrated that human PAR-1 and PAR-2 genes are contained within YAC 798D11 and separated maximally by ~100 kb (11). In an attempt to identify additional PARs that potentially may be clustered in this region of the genome, differential genomic blotting was adapted using a series of cDNA probes encompass-

[2] Stanford Human Genome Center (http://shgc.www.stanford.edu/rh) (1996).

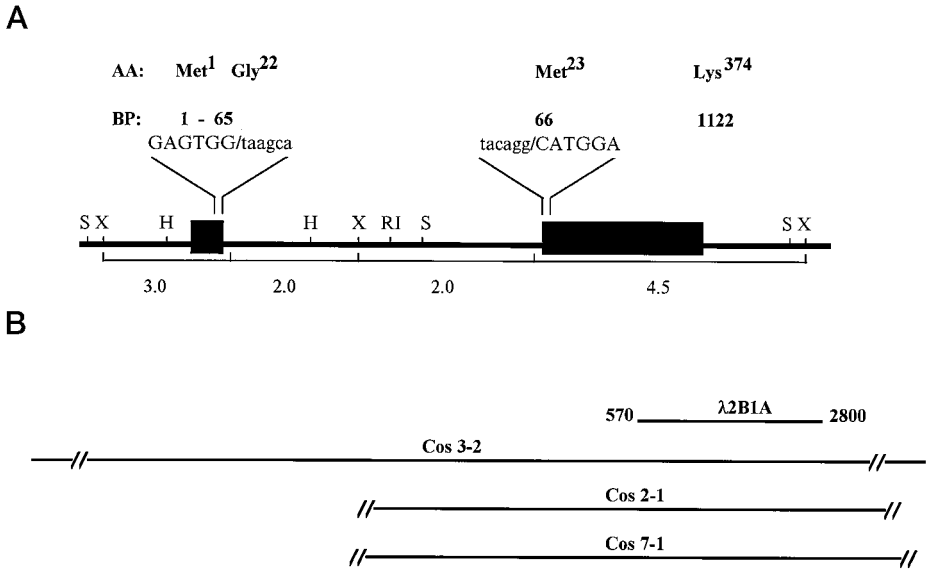

FIG. 4. **Schema outlining the structural organization of the PAR-3 gene.** *Panel A*, exons are indicated by *solid rectangles*, and distances (in kb) with key restriction enzymes are denoted (*X*, *Xba*I; *H*, *Hin*dIII; *RI*, *Eco*RI; *S*, *Sph*I). The splice junction sites are delineated (exon sequences are *capitalized*) along with the nucleotides and amino acid residues contained in each exon. The numbering system empirically starts with the initiator methionine (ATG = +1). *Panel B*, the schema of the overlapping cosmid clones used to characterize the PAR-3 gene and the PAR-3 cDNA clone λ2B1A isolated and characterized from the HUVEC cDNA library.

ing distinct regions of the PAR-1 or PAR-2 genes. Using such an approach, PAR-1-specific probes failed to identify any novel cross-hybridizing fragments (not shown). In contrast, a PAR-2-specific probe encompassing the 5′-region of the cDNA identified a novel band at low stringency which was not evident when the blot was washed at higher stringency (Fig. 1). By inversion field gel electrophoresis, this *Eco*RI fragment was estimated to be ~16 kb and could not be resolved by the known genomic organization of PAR-2 (5). Furthermore, this band was not present within a P1 genomic clone (P1142) shown previously by Nystedt and colleagues (5) to contain the entire PAR-2 gene (not shown), again strongly suggesting that it represented a previously uncharacterized, homologous PAR or a processed pseudogene. Concomitant with these initial observations, a routine BLAST (21) homology search using PAR-2 sequences identified a highly homologous expressed sequence tag (EST) AA177828, partially characterized from a murine splenic cDNA library, as part of the Washington University/HHMI Mouse EST project. This expressed sequence tag was purchased from Research Genetics, fully sequenced, and found to contain a 1,238-bp insert encoding a 283-amino acid open reading frame (representing an incomplete cDNA) demonstrating highest homology to PAR-1 and PAR-2. This ^{32}P-radiolabeled insert was then used to screen empirically a HUVEC cDNA library using low stringency screening to maximize hybridization cross-species, with the isolation of three cDNA clones, the longest of which (λ2B1A, 2,566 bp) was characterized more fully (see below). As demonstrated in Fig. 1*D*, this cDNA (now known to be identical to PAR-3) (10), cross-hybridized to the novel ~16-kb *Eco*RI fragment recognized by the 5′-PAR-2 probe (Fig. 1*C*), thereby establishing its identity as the human PAR-3 gene.

Physical and Genetic Mapping within the PAR Gene Cluster—To establish more precisely distances among the PAR genes within this genomic segment, we completed genetic mapping using radiation hybrid mapping panels (11, 14). Using the lower resolution G3 panel, the amplification (and retention) patterns for all three genes were indistinguishable (no breaks were observed in the 83 hybrids typed), establishing that the closest framework marker to all three PARs was D5S424 (22), with significant linkage as well to D5S1977, D5S2529, and D5S2596 (in order of decreasing log of odds scores, see Fig. 2). Thus, all three PARs were linked tightly to the identical microsatellite markers and were at least as close to each other as the resolution power of this panel (360–500 kb).[2] To establish further interorder assignments and distance, we determined amplification patterns from a second radiation hybrid panel TNG3 with a higher lengthwise resolution of ~100 kb (11).[2] The amplification patterns obtained using this RH panel were analyzed using RH2PT (16) and demonstrated that the three genes could now be resolved, with the likely order *centromere*–D5S424–PAR-2–PAR-1–PAR-3–*telomere* (Fig. 2). Although physical conversions are not available for the TNG3 RH panel, if one assumes an average resolution of 3–6 kb/centiRad throughout the panel,[2] this initial analysis suggested that the three PARs are separated by ~110 to ~220 kb, which was confirmed subsequently by inversion field gel electrophoresis and Southern blot analysis. DNA digests of YAC 798D11 were completed using various restriction endonucleases (including rare-cutting enzymes) in an attempt to resolve the three genes within single large genomic fragments. As revealed in Fig. 3, Southern blot analysis demonstrated that all three cDNAs were contained within restriction fragments of ~90 kb (*Xho*I) or ~120 kb (*Not*I), consistent with a distance among the genes of less than 100 kb.

PAR-3 Genomic Characterization—To characterize the genomic structure of PAR-3, a cosmid library was constructed using YAC 798D11 DNA. Approximately 7×10^3 independent clones from the unamplified library were screened using the PAR-3 cDNA, with the identification of 10, three of which (COS3–2, COS2–1, and COS7–1) were characterized further. Only one of the three clones (COS3–2) contained the entire PAR-3 gene, whereas COS2–1 and COS7–1 lacked the 5′-coding region (Fig. 4). PAR-3 exons, intron/exon boundaries, and portions of the flanking introns were sequenced bidirectionally for further analysis. Not unexpectedly, PAR-3 displayed a genomic organization similar to that of the PAR-1/PAR-2 genes (5, 9, 23), containing a small first exon and a larger second exon encoding the majority of the coding sequence and the protease cleavage site. The single intronic splice site occurs after the second nucleotide of the Gly^{22} codon, indicative of a type II splice site, although the splice junction sequences are somewhat atypical (24). Nucleotide analysis of the entire coding sequence was identical to that described initially (10), with the identification of an additional 1,451 bp of 3′-untranslated sequence in the cDNA clone λ2B1A. This sequence has been deposited into the GenBank data base and assigned the accession number AF053124. The size of the PAR-3 first intron was estimated at ~4 kb, utilizing restriction mapping and long range PCR from YAC 798D11, COS3–2, and total human

A

```
-1214  GAGGTTTCGCAGTCATTTTTTCTGGCATNTCCTANCTTAGTTTCAGGGGA  -1165
-1164  AATTGGATTTTCGGATTCTTGCGGCATTTGTAAAAGAGCAGGCTGGTGGG  -1115
-1114  ATGTTCAGGCTTCAAGTTTAAAGTTTTATTAACAACAGAAAAATGTGTTA  -1065
-1064  TAATGCATTTTTTTTAACNGTATATTAAGTCATAACTTCAACAGAATATT  -1015
                HindIII
-1014  ACAATTCATAAAAGCTTATATGTTGTACAACAATGTGAATTGTATTTAAC  -965
 -964  ATTACTGAACTGTAACAACTTAATACTGGTTAAGATAGTAAATTTTATGT  -915
 -914  TACGTATATTTTACCACTATTAAAAATATCTTATTGTAGACTTATTCACC  -865
 -864  AACACTCATGGAATAAAGGGAGTCCTCATTTTCATGATGTGCTATGATTT  -815
 -814  TAGTTTAACTGAACAGCGTTGTTTGGGAGGTTCCTCCAGTTATCTGACCC  -765
 -764  TAAGGGTTATTGAATGGCTCAAAACACATCAAGATAAGGCAAAAAAAAAA  -715
 -714  AAAAAAAGCCTGAACAAACGCCATCTTCACCCGGGGAAGAAAAACCACCA  -665
 -664  CCACTCAAAAGCCAGTTCTGGCCAGGCACTGACGACAAACTGAAATCAAT  -615
 -614  ATAACACTGATAGAAAATTTTCAAAGTGATTCACTGCTCAATTTGAATTT  -565
 -554  TCTTAAAAGTTTGTTTTCCATGATTAATTTATAATTATGTAAAGTGTTTA  -515
 -514  AGGATTAAGATTTGAAATAGCTGGGAAGATAAAGGAAAGGATAATTTATT  -465
 -464  AAGTAGAAATTACACTCTGGAACTGCATTTTTAAAACGGATAAGAAATGA  -415
 -415  AATGTGGGACAGATTCAAAACTTACTGCTGTTCAACATCTGTTTTTGGCT  -365
 -364  TAGTTCTGTAAAGGCCTGTGTAATTTCTGCCATTCTTTAAAAGCAAATCT  -315
 -314  ACTAGGGGAGAATTACAGCACCTATTCAGAATAGATTGTTGGGGGTGGGT  -265
 -264  AAGAGTTAAATGCCTTTCTCCAGGGATAACGTAACACGTTCAGAGGCTTG  -215
 -214  GCCTGAGTCATGCTTACTGAAGCATCGAGTGGATTACATCCTTTCCCCTG  -165
                ⇐
 -164  CGGAGGACCAGGGCAAGTTTCCTGCCTGCACGGCACAGGAGAGCAAACTT  -115
 -114  CTACAGACAGACCAAGGCTTCCATTTGCTGCTGACACATGGAACTGAGGT  -65
  -64  GAAATTGTGCTCCATGATTTTACAGATTTCATAACGTTTAAGAGACGGGA  -15
  -14  CTCAGGTCATCAAA                                      -1
```

B

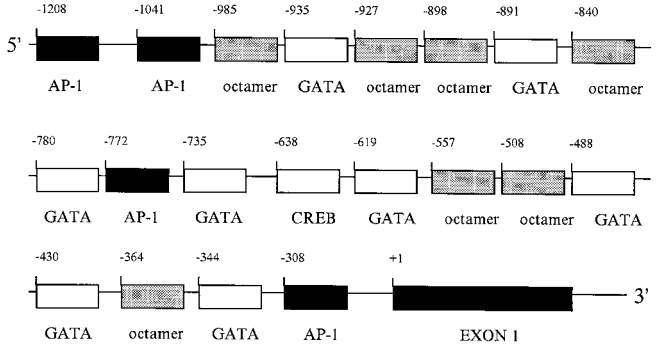

FIG. 5. **Nucleotide analysis of the PAR-3 5′-flanking regions.** *Panel A*, the 5′-regulatory sequence is displayed, with the start of the previously unpublished sequence depicted by the *arrow* and the key *Hin*dIII restriction site delineated. *Panel B*, the schema summarizes the putative transcriptional regulatory sequences.

genomic DNA. Thus, although genomic rearrangements/deletions are not uncommonly found in YACs, the identical sizes of restriction fragments and PCR fragments confirm these size estimates and determinations.

A ~5-kb *Xba*I fragment containing the first exon and 5′-untranslated region (see Fig. 4) was sequenced bidirectionally to characterize further potential regulatory sequences involved in PAR-3 expression (Fig. 5). Neither a TATA box nor CCAAT sequences are evident (25), similar to the promoter analysis of the PAR-1 gene (9). Although GC-rich regions (SP1 binding sites) potentially involved in transcriptional regulation of housekeeping genes are not found infrequently in TATA-less promoters (and present in the PAR-1 promoter, for example (9,

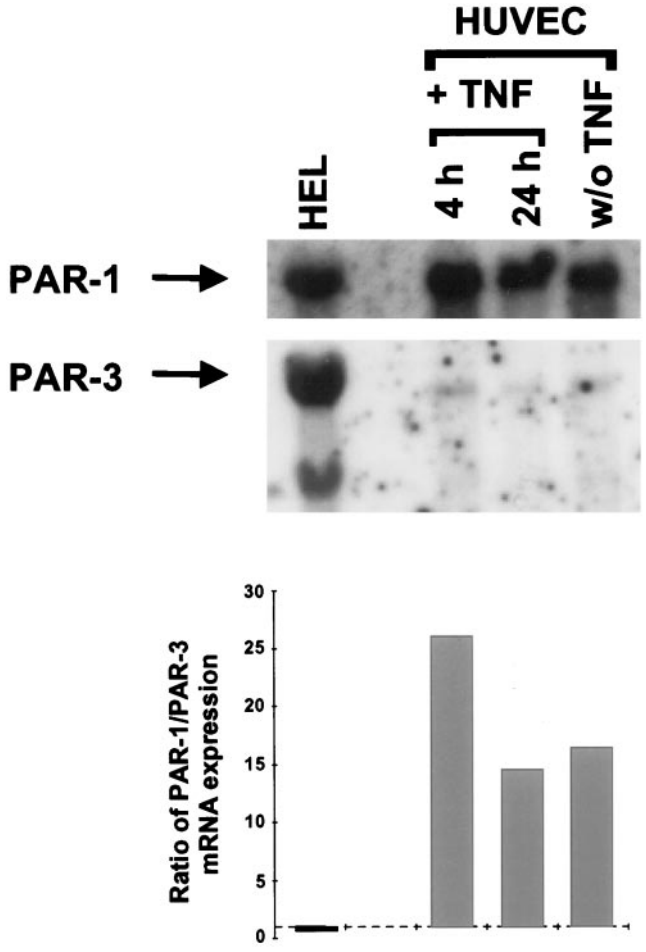

FIG. 6. **PAR-3 mRNA expression.** 10 μg of total cellular RNA (HEL) or 1 μg of poly(A) RNA (HUVEC, with or without 100 units/ml tumor necrosis factor-α (*TNF*), was sized fractionated in a 1% denaturing agarose gel, transferred to nylon membranes, and hybridized sequentially with ^{32}P-radiolabeled PAR-3 or PAR-1 cDNA. Blots were washed at high stringency and analyzed by autoradiography after a 3-day exposure. Two PAR-3 transcripts of ~4.0 kb and ~2.0 kb are evident in HEL cells, as demonstrated previously (10), whereas the single PAR-1 transcript is evident (*upper panel*). In HUVEC, only larger transcript is identified with this exposure. Densitometric scanning was used to quantify relative PAR-1/PAR-3 (4.0-kb transcript) expression (*lower panel*).

25)), such sequences are absent in the PAR-3 gene 5′-regulatory sequences, further suggesting transcriptional regulation by more restricted nuclear binding elements. Further analysis of the 5′-regulatory region (Fig. 5*B*) demonstrated potential *cis*-acting DNA elements, such as AP-1-like elements present at −772, −1041, and −1208 (26, 27), and a single cAMP response element-binding protein (28) sequence present at −638. Eight GATA-like sequences known to represent binding sites for the erythroid nuclear factor protein NF-E1 are present at −344, −430, −480, −619, −735, −891, and −935 (29). This protein is also known to be expressed in megakaryocytes (30), an observation of potential relevance given the observed high level of PAR-3 expression in these cells (10; see below). Also of relevance for megakaryocytic gene regulation is the presence of seven distinct octameric sequences, regulatory elements known to modulate the expression of various megakaryocyte genes (31, 32).

PAR-3 mRNA Expression in Endothelial Cells—Initial evaluation for PAR-3 transcript expression was pursued by Northern blot analysis using murine tissues. Dual transcripts of ~4.0 and ~2.0 kb were evident primarily in poly(A) mRNA from spleen, with little to no expression evident in poly(A) mRNA

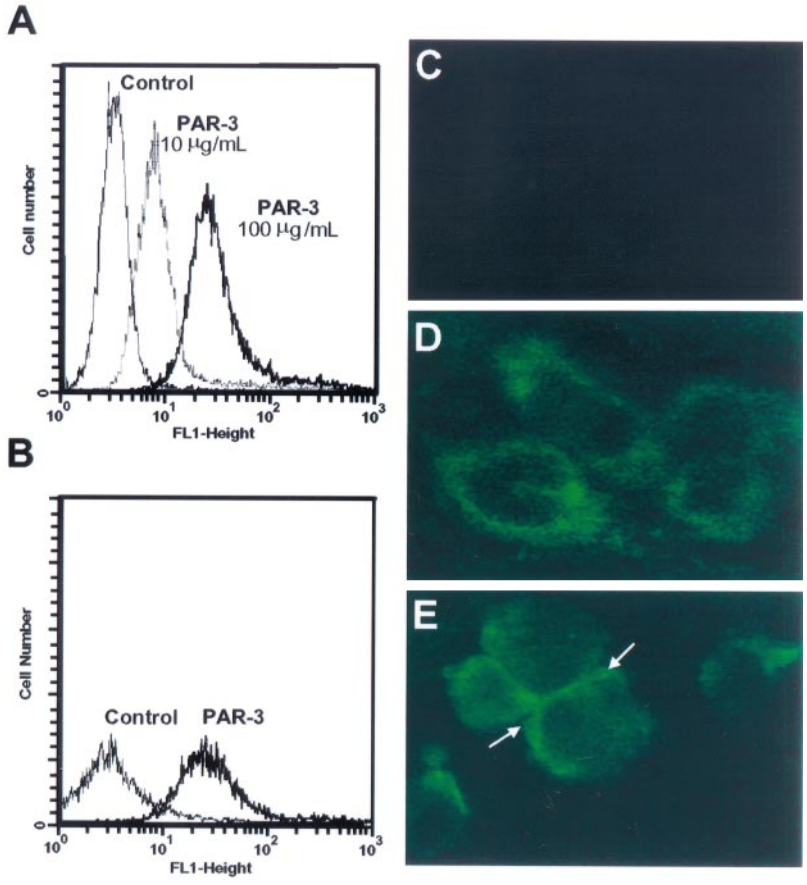

FIG. 7. **HUVEC PAR-3 immunodetection.** *Panel A*, the FITC-conjugated anti-PAR-3 IgG (at various concentrations) or a 1:100 dilution of the FITC-conjugated IgG alone (control) was incubated with 1×10^6 HEL cells for 60 min at 4 °C before analysis by flow cytometric analysis, with evidence for optimal antibody reactivity at 100 μg/ml. *Panel B*, endothelial cells were detached, and 1×10^5 endothelial cells were incubated with 100 μg/ml FITC-conjugated anti-PAR-3 IgG (or the secondary antibody alone) for 60 min at 4 °C followed by flow cytometry for evaluation of cell surface receptor expression. *Panels C–E*, endothelial cells were grown until confluent, serum starved for 1 h, and then fixed and permeabilized using ice-cold acetone for 60 s (*panels C* and *D*) or fixed without permeabilization using 4% paraformaldehyde (*panel E*) before immunofluorescence staining using 100 μg/ml FITC-conjugated anti-PAR-3 IgG, as outlined under "Materials and Methods." Distinct intracellular staining is evident in *panel D*, whereas cell surface staining is seen in nonpermeabilized cells (*panel E*). Note the stippled staining patterns consistent with cell surface expression and the more intense staining in areas of cell-cell contact (*panel E*, *arrows*). No staining is seen using the secondary antibody alone (*panel C*). Final magnification in all panels is × 1100.

from brain, kidney, liver, lung, pancreas, or smooth muscle (not shown), results that were consistent with those described previously (10). Interestingly, this initial analysis suggested that PAR-3 may be expressed in tissues of hematopoietic origin, and cellular sources for PAR-3 expression were pursued subsequently in megakaryocytes/platelets and endothelial cells. The latter cell type was studied because of prior evidence for both PAR-1 and PAR-2 expression in endothelial cells (6) and strong presumptive evidence for PAR-3 expression obtained during initial HUVEC cDNA library screening (see above). Accordingly, Northern blot analysis was completed using total cellular RNA from endothelial cells and from HEL cells, which display phenotypic features of megakaryocytic differentiation (33). As shown in Fig. 6, PAR-3 transcripts were clearly evident in HEL cells, approximately 2-fold higher than those of PAR-1 transcripts. In contrast, although PAR-3 expression was evident in HUVEC, the relative transcript expression was considerably less than that of PAR-1, with steady-state PAR-1 levels nearly 25-fold greater than those of PAR-3. To address the possibility that PAR-3 expression could be up-regulated during cell activation, cells were then stimulated with the endothelial cell stimulant tumor necrosis factor-α, and differential PAR-1/PAR-3 expression was studied further. Minimal change in either transcript expression was evident, with the PAR-1/PAR-3 ratio remaining skewed toward enhanced PAR-1 expression at both time points studied.

The evidence for PAR-3 transcript expression in endothelial cells prompted further studies to elucidate receptor expression in these cells. For these studies, a PAR-3 peptide spanning the thrombin cleavage site was synthesized for generation of a polyclonal antibody, and its immunoreactivity with the synthetic peptide was confirmed by enzyme-linked immunosorbent assay. To enhance the detection of apparently low level endothelial cell PAR-3 expression as determined by Northern analysis (Fig. 6), the purified anti-PAR-3 IgG was coupled to FITC before subsequent immunofluorescent staining in HUVEC. As shown in Fig. 7*A*), this antibody was optimally immunoreactive with PAR-3 on HEL cells at a concentration of 100 μg/ml, an antibody concentration that was used for evaluation of PAR-3 expression in HUVEC. Consistent with the results demonstrated by Northern blot analysis, cell surface PAR-3 expression was readily evident on vascular endothelial cells as determined by flow cytometry (Fig. 7*B*). The cellular distribution of PAR-3 was then pursued directly by immunofluorescent staining (Fig. 7*C–E*) and was consistent with both an intracytoplasmic and cell surface pool of receptors. This similar pattern has been described both for endothelial cell PAR-1 and PAR-2 and has been postulated to represent a mechanism of regulating cell surface PAR expression and responsiveness in these cells (6, 34). Interestingly, the pattern of cell surface immunofluorescence appeared to demonstrate more intense PAR-3 expression in areas of endothelial cell-cell contact. Although the significance of this remains unclear at this time, it may suggest an undefined role for PAR-3 in these cells, possibly distinct from that mediating cell activation events through receptor proteolysis.

Platelet PAR-3 Expression—As described initially, PAR-3 transcripts were expressed prominently in splenic megakaryocytes as evaluated by *in situ* hybridization (10). This observation, combined with our demonstration for considerable PAR-3 expression in the megakaryocyte-like HEL cells, prompted us to study PAR-3 expression in platelets, an issue of considerable importance given previous evidence for dual thrombin receptors or signaling pathway(s) in these cells (20, 35). As shown by reverse transcription-PCR, a PAR-3 mRNA transcript was readily detectable in human platelets (Fig. 8). Because this assay as designed was not quantitative, cell surface receptor expression was then studied by flow cytometric analysis, de-

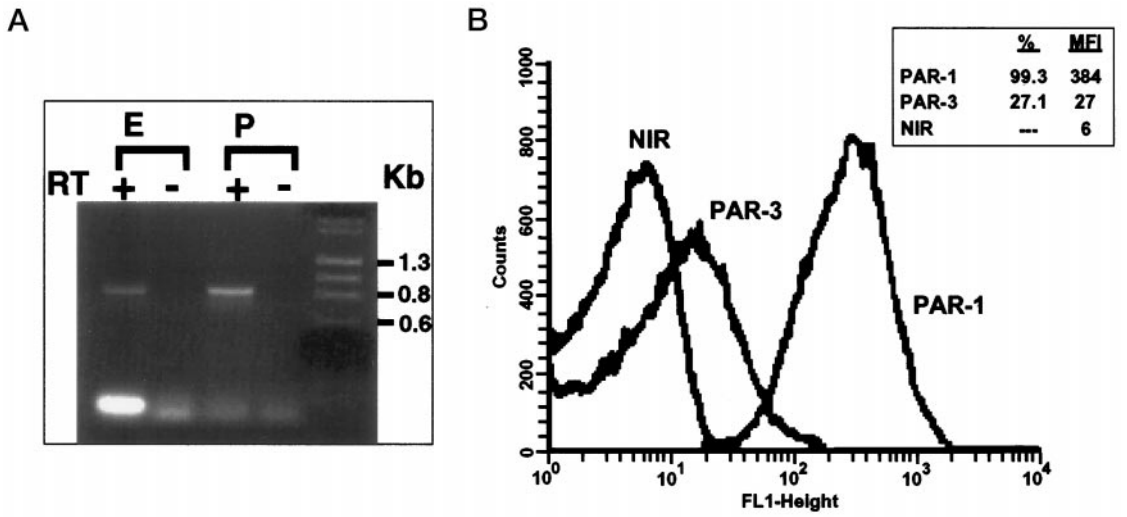

FIG. 8. **PAR-3 expression in human platelets.** *Panel A*, reverse transcriptase-PCR using total cellular RNA from endothelial cells (*E*) or platelets (*P*) was completed as outlined under "Materials and Methods" in the presence (+) or absence (−) of reverse transcriptase (*RT*), followed by PCR using PAR-3 oligonucleotide primers PAR2065 and PAR2066. As shown, a single band of the anticipated size (878 bp) was evident in both cells only in the presence of reverse transcriptase, confirming PAR-3 mRNA expression in these cells. *Panel B*, flow cytometric analysis of human platelets was completed using 100 μg/ml FITC-conjugated anti-PAR-3, anti-PAR-1, or nonimmune rabbit (*NIR*) IgG, followed by immunodetection (for PAR-1 and NIR) using a 1:100 dilution of the FITC-conjugated $F(ab')_2$ secondary antibody. The percent positive cells and the mean fluorescence intensity (*MFI*) (*inset*) were standardized against the nonimmune IgG/FITC control. The results demonstrate detectable but modest levels of cell surface PAR-3 expression compared with that of PAR-1. Identical results were obtained from two volunteers studied on different days.

signed to elucidate more accurately relative PAR-1/PAR-3 expression on the platelet cell surface. Interestingly, these results are comparable to those seen in HUVEC, demonstrating detectable but low level PAR-3 expression and considerably less cell surface receptor when compared with PAR-1. Prior determinations suggest that there are approximately 1,500–2,000 PAR-1 receptors on human platelets (36, 37). Based on the relative mean fluorescence intensities of PAR-1/PAR-3 as established by flow cytometry, we would estimate PAR-3 receptor density to be approximately 10% of PAR-1 (~150–200 receptors/platelet), although definitive comparisons will ultimately require monoclonal antibodies with limited antigenic epitopes.

Summary and Implications for Future Research—PARs represent a unique and rapidly emerging family of G protein-coupled seven-transmembrane receptors that mediate cell activation events to serine proteases generated during one of three major protease-generating pathways in humans (inflammatory, fibrinolytic, or hemostatic). To date, all three PAR genes have been identified as being structurally conserved and residing within a discrete segment of the human genome, strongly suggesting evolution from a common ancestral gene. Given progressive evidence that a larger number of serine proteases affect cell activation (2), we would speculate that more structurally similar receptors exist, some of which may be found within this gene cluster or identified as part of the human genome initiative. The construction of a cosmid library containing the repertoire of genes encompassing this region of the genome may facilitate the search for, and rapid characterization of, other structurally similar receptors that may colocalize within this region of the genome.

What is the function of PAR-3? Although characterized initially as a second thrombin receptor (10), the Lys^{38}/Thr^{39} cleavage site appears somewhat unusual for a thrombin substrate. Nonetheless, this may represent the alternative thrombin-responsive pathway described previously in multiple cells, including platelets (20, 35) and endothelial cells (20). In human platelets, PAR-1 is the primary regulator of platelet aggregation to thrombin (15); and in both platelets and endothelial cells, anti-PAR-1 antibodies abrogate the immediate phase of intracytosolic calcium release, although a moderate and sustained response remains evident (20). Although PAR-3 is clearly expressed in both of these cells by mRNA and protein determinations, the levels appear modest compared with those of PAR-1. Interestingly, PAR-3 expression appears considerably higher in megakaryocytes (10) and in the megakaryocyte-like cell line (HEL) studied as our model system. Thus, we would speculate that activation of human platelet PAR-3 by α-thrombin (or other unidentified proteases) may be less important for physiological responses in these mature cells but potentially more applicable for poorly defined cellular responses (to proteases) that may regulate megakaryocytic (or endothelial cell) development.

Acknowledgments—We thank Shirley Murray for assistance with the processing of this manuscript, Dr. Barry Coller for assistance and advice with antibody generation and for critically reviewing the manuscript, and David Colflesh for assistance with the fluorescent microscopy and image analysis.

REFERENCES

1. Bahou, W. F., and Schmidt, V. A. (1996) *Platelets* **7,** 253–260
2. Hollenberg, M. D. (1996) *Trends Pharmacol. Sci.* **17,** 3–6
3. Vu, T., Hung, D., Wheaton, V., and Coughlin, S. (1991) *Cell* **64,** 1057–1068
4. Nystedt, S., Emilsson, K., Wahlestedt, C., and Sundelin, J. (1994) *Proc. Natl. Acad. Sci. U. S. A.* **91,** 9208–9212
5. Nystedt, S., Emilsson, K., Larsson, A. K., Strombeck, B., and Sundelin, J. (1995) *Eur. J. Biochem.* **232,** 84–89
6. Mirza, H., Yatsula, V., and Bahou, W. F. (1996) *J. Clin. Invest.* **97,** 1705–1714
7. Mirza, H., Schmidt, V., Derian, C., Jesty, J., and Bahou, W. (1997) *Blood* **90,** 3914–3922
8. Chambard, J., Paris, S., L'Allemain, G., and Pouyssegur, J. (1987) *Nature* **326,** 800–803
9. Schmidt, V. A., Vitale, E., and Bahou, W. F. (1996) *J. Biol. Chem.* **271,** 9307–9312
10. Ishihara, H., Connolly, A. J., Zeng, D., Kahn, M. L., Zheng, Y. W., Timmons, C., Tram, T., and Coughlin, S. R. (1997) *Nature* **386,** 502–506
11. Schmidt, V. A., Nierman, W. C., Feldblyum, T. V., Maglott, D. R., and Bahou, W. F. (1997) *Br. J. Haematol.* **97,** 523–529
12. Pustell, J., and Kafatos, F. (1986) *Nucleic Acids Res.* **14,** 479–488
13. Quandt, K., Frech, K., Karas, H., Wingender, E., and Werner, T. (1995) *Nucleic Acids Res.* **23,** 4878–4884
14. Cox, D. R., Burmeister, M., Price, E. R., Kim, S., and Myers, R. M. (1990) *Science* **250,** 245–250
15. Hoxie, J. A., Ahuja, M., Belmonte, E., Pizarro, S., Parton, R., and Brass, L. F. (1993) *J. Biol. Chem.* **268,** 13756–13763
16. Boehnke, M., Lange, K., and Cox, D. R. (1991) *Am. J. Hum. Genet.* **49,** 1174–1188
17. Read, M. A., Whitley, M. Z., Gupta, S., Pierce, J. W., Best, J., Davis, R. J., and Collins, T. (1997) *J. Biol. Chem.* **272,** 2753–2761
18. Ponte, P., Gunning, P., Blau, H., and Kedes, L. (1983) *Mol. Cell. Biol.* **3,**

1783–1791
19. Newman, P., Gorski, J., White, G., Gidwitz, S., Cretney, C., and Aster, R. (1988) *J. Clin. Invest.* **82,** 739–743
20. Bahou, W., Coller, B., Potter, C., Norton, K., Kutok, J., and Goligorsky, M. (1993) *J. Clin. Invest.* **91,** 1405–1413
21. Altschul, S. F., Gish, W., Miller, W., Myers, E. W., and Lipman, D. J. (1990) *J. Mol. Biol.* **215,** 403–410
22. Dib, C., Faure, S., Fizame, C., Samson, D., Dourot, N., Vignal, A., Millasseau, P., Marc, S., Hazan, J., Seboun, E., Lathrop, M., Gyapay, G., Morissette, J., and Weissenbach, J. (1996) *Nature* **380,** 152–154
23. Li, F., Baykal, D., Horaist, C., Yan, C.-N., Carr, B. N., Rao, G. N., and Runge, M. S. (1996) *J. Biol. Chem.* **271,** 26320–26328
24. Mount, S. (1982) *Nucleic Acids Res.* **10,** 459–472
25. Bucher, P. (1990) *J. Mol. Biol.* **212,** 563–578
26. Lee, W., Mitchell, P., and Tjian, R. (1987) *Cell* **49,** 741–752
27. Mignotte, V., Eleouet, J. F., Raich, N., and Romeo, P.-H. (1989) *Proc. Natl. Acad. Sci. U. S. A.* **86,** 6548–6552
28. Quinn, P. G. (1993) *J. Biol. Chem.* **268,** 16999–17009
29. Pevny, L., Simon, M. C., Robertson, E., Klein, W. H., Tsai, S., D'Agati, V., Orkin, S. H., and Constantini, F. (1991) *Nature* **349,** 257–260
30. Martin, D. I., Zon, L. I., Mutter, G., and Orkin, S. H. (1990) *Nature* **344,** 444–447
31. Villa-Garcia, M., Li, L., Riely, G., and Bray, P. F. (1994) *Blood* **83,** 668–676
32. Staudt, L. M., Clerc, R. G., Singh, H., LeBowitz, J. H., Sharp, P. A., and Baltimore, D. (1988) *Science* **241,** 577–580
33. Long, M. W., Heffner, C. H., Williams, J. L., Peters, C., and Prochownik, E. V. (1990) *J. Clin. Invest.* **85,** 1072–1084
34. Hung, D. T., Wong, Y. H., Vu, T. K., and Coughlin, S. R. (1992) *J. Biol. Chem.* **267,** 20831–20834
35. McGowan, E. B., and Detwiler, T. (1986) *J. Biol. Chem.* **261,** 739–746
36. Brass, L. F., Vassallo, R. R., Jr., Belmonte, E., Ahuja, M., Cichowski, K., and Hoxie, J. A. (1992) *J. Biol. Chem.* **267,** 13795–13798
37. Norton, K. J., Scarborough, R. M., Kutok, J. L., Escobedo, M. A., Nannizzi, L., and Coller, B. S. (1993) *Blood* **82,** 2125–2136